Applied Catalysis A: General 452 (2013) 179–188

Contents lists available at SciVerse ScienceDirect

Applied Catalysis A: General

journal homepage: www.elsevier.com/locate/apcata

Synthesis of Ni/Al_2O_3 and $Ni–Co/Al_2O_3$ coatings onto AISI 314 foams and their catalytic application for the oxidative dehydrogenation of ethane

J.P. Bortolozzi, L.B. Gutierrez, M.A. Ulla*

Instituto de Investigaciones en Catálisis y Petroquímica, INCAPE, (FIQ, UNL-CONICET), Santiago del Estero 2829, 3000 Santa Fe, Argentina

ARTICLE INFO

Article history:
Received 4 October 2012
Received in revised form
22 November 2012
Accepted 23 November 2012
Available online xxx

Keywords:
Structured catalyst
AISI 314 foam
Ni/Al_2O_3
$Ni–Co/Al_2O_3$
Oxidative dehydrogenation

ABSTRACT

The aim of this work was to obtain alumina-supported Ni and Ni–Co oxide catalytic coating onto an AISI 314 foam (60 ppi) so as to produce a good distribution of the catalytic components and reproduce characteristics of their interactions similar to those observed in the powder catalysts. These catalytic systems were characterized by different techniques (Laser Raman spectroscopy, X-ray diffraction, temperature-programmed reduction, scanning electron microscopy and energy-dispersive X-ray analysis). The oxidative dehydrogenation of ethane was used as test reaction. The results indicated that the Ni and $Ni–Co/Al_2O_3$ powder catalysts were active and selective for this reaction. For the active metal loading used (15 wt%), the addition of cobalt with an atomic ratio of Co/Ni = 0.114 slightly improved the ethylene productivity, possibly due to the enhancement of Ni dispersion. However, the addition of a higher amount (Co/Ni = 0.253) led to a lower productivity, probably due to the presence of cobalt compounds and to the increase in the NiO crystal size. The structured systems showed a performance similar to that of the corresponding powder forms and they also showed good adhesion of the catalytic layer onto the metallic foams.

The features of the resulting structured systems are very sensitive to the variables which involve the deposition method. Therefore, it is necessary to take into account the control of such parameters in order to obtain good, repetitive depositions of the active components and a correct distribution of the support in the coverage. In the same sense, the achievement of a constant relationship between the active metals is significant because, otherwise, the activity and selectivity of these systems could be affected.

1. Introduction

Structured catalysts are currently used in numerous chemical reactions because they have improved the global efficiency in a variety of processes. These catalysts may consist of either a substrate which acts as a catalyst or a catalytic formulation deposited as a thin film onto an inert matrix [1].

In the last few years, metallic foams have become popular as substrates for this type of catalysts. Their interesting properties such as low density, high porosity and better coefficients associated with transport phenomena make them attractive for different applications such as partial oxidation of alcohols [2], methane reforming [3] and elimination of soot and purification of pollutants from diesel engines exhaust gases [4], among others.

Mechanical strength and high thermal conductivity [5] are other advantages of these materials. The latter feature allows more uniform temperature profiles throughout the structure avoiding the drawbacks associated with the generation of "hot spots". Additional benefits include high energy and mass transfer coefficients [6,7] and the possibility of obtaining turbulent flow regimes, with high radial dispersion. These characteristics promote a better mixing of the reagents stream.

In order to modify the surface conditions of this type of structures some treatments have been applied [8–10]. Among them, the thermal treatments applied to stainless steel foams allow generating a stable, sufficiently rough film, which facilitates the suitable anchorage of a catalytic formulation [11].

On the other hand, light olefins, especially ethylene, have become compounds of great industrial interest since they are key intermediates in the production of valuable products such as polymers and fibers. Nowadays, they are mostly produced by steam cracking of certain petroleum fractions such as naphtha or ethane. According to the energy requirements, this is the most demanding process of the chemical industry. Other routes like methane-based or the oxidative coupling of methane have been proposed but they are not economically feasible or they evoke high

* Corresponding author. Tel.: +54 342 4536861; fax: +54 342 4536861.
E-mail address: mulla@fiq.unl.edu.ar (M.A. Ulla).

0926-860X/$ – see front matter © 2012 Elsevier B.V. All rights reserved.
http://dx.doi.org/10.1016/j.apcata.2012.11.036

CO_2 emissions [12]. The high cost of the energy needed to reach severe operating conditions and the constant growth in market demands are motivations for finding new production processes, designed to achieve better performance and less power consumption.

An innovative, potentially attractive alternative to produce large-scale olefins is the oxidative dehydrogenation of hydrocarbons, mainly due to the simplicity of the process and the exothermic nature of the reactions involved that allow a better energy balance [13].

Heracleous et al. have studied nickel alumina-supported catalysts [14] with the addition of a variety of promoters applied to this reaction. The work concludes that the presence of alumina modifies the electronic properties of NiO making it selective toward ethylene. Solsona et al. [15] recently reported results about NiO supported on mesoporous alumina and γ-alumina containing tungsten as promoter. The results suggest that the good catalytic performance could be related to the high dispersion of NiO, which could favor the elimination of non-selective sites. However, the authors think that a deeper study of the Ni–W–O system is needed [15].

Then, supported nickel oxide is presented as an attractive option to be considered due to both its low cost and good properties to activate ethane at relatively low temperatures. This latter point and the importance of depositing the catalyst onto a substrate are essential topics if potential industrial applications of these processes are to be considered. It is also evident that greater efforts should be devoted to the study of catalysts and reactor configurations with the purpose of improving catalyst lifetime, stability and energy consumption.

In this work, alumina-supported Ni and Ni–Co oxide catalysts in powder and structured forms were prepared. Their physicochemical characterization was performed using Laser Raman spectroscopy (LRS), X-ray diffraction (XRD), temperature-programmed reduction (TPR), scanning electron microscopy (SEM) and energy-dispersive X-ray analysis (EDX). The oxidative dehydrogenation of ethane was used as test reaction in order to further study the distribution of the active species. The aim of this work was to obtain alumina-supported Ni and Ni–Co oxide catalytic coating onto metallic foams (60 ppi) so as to produce a good distribution of the catalytic components and reproduce characteristics of their interactions similar to those observed in the powder catalysts.

2. Experimental

2.1. Structured catalysts

AISI 314 stainless steel foams (Porvair®, 60 ppi) were treated in a muffle at 900 °C for 2 h. The γ-Al_2O_3 support (Nyacol® AL20DW) was deposited by vacuum-assisted immersion and calcined in static air at 700 °C for 2 h. Solutions of the metallic oxide precursors, $Ni(NO_3)_2{\cdot}6H_2O$ and $Co(NO_3)_2{\cdot}6H_2O$, were used to incorporate the active metallic oxides to the alumina coating by cycles of immersion–blowing–drying–calcination. This cycle was repeated until the final metal oxide loading of 15 wt% was achieved. For this proposal, two different concentrations were prepared: 0.85 M (concentrated solution – CS) or 0.43 M (dilute solution – DS) solutions. The excess was removed by blowing and then dried in an oven at 120 °C for 1 h. The catalytic systems were finally calcined in air flow at 550 °C for 4 h.

The structured catalysts were also prepared in NiO and Ni–Co oxide forms. For the latter, the precursor solutions were prepared with Co/Ni atomic ratios 0.114 and 0.253. The catalysts were designated as indicated in Table 1.

2.2. Powder catalysts

NiO, CoO_x and Ni–Co oxide catalysts were prepared by wet impregnation and co-impregnation, respectively, with a 15 wt% maximum metal loading. The support was γ-Al_2O_3 PURALOX Condea SBA 230. Aqueous solutions of $Ni(NO_3)_2{\cdot}6H_2O$ (0.43 M) and $Co(NO_3)_2{\cdot}6H_2O$ (0.05 M) were used as metallic precursors. Two different Co/Ni atomic ratios (0.114 and 0.253) were used in the mixture of these precursors. The volume of each solution used for the impregnation process was determined to obtain the selected metal loading. The solvent was removed by evaporation and the resulting powders were dried in a stove at 120 °C for 8 h and finally calcined in air flow at 550 °C for 4 h. The catalysts were designated as indicated in Table 1.

2.3. Catalysts characterization

The Raman spectra were recorded using a LabRam spectrometer (Horiba-Jobin-Yvon) coupled to an Olympus confocal microscope (a 100× objective lens was used for simultaneous illumination and collection), equipped with a CCD detector cooled to about −70 °C using the Peltier effect. The excitation wavelength was in all cases 532.13 nm (Spectra Physics diode pump solid state laser). The laser power was set at 30 mW.

The powder catalyst surface areas were measured by N_2 adsorption (−196 °C) with a Quantachrome Autosorb-1 equipment. The multipoint BET method was used. Before the experiments, the powders were treated in vacuum at 250 °C for 3 h.

Crystalline phases of the different powder catalysts were studied by X-ray diffraction (XRD). The analysis was performed with a Shimadzu XD-D1 diffractometer. Diffraction patterns were recorded using Cu–Kα radiation over a 20–85° range at a scan rate of 1°/min, operating at 30 kV and 40 mA. The software package of the equipment was used for the identification of the phases. The estimated size of nickel oxide crystals was calculated by the Scherrer equation.

The reducibility of nickel and cobalt species for the powder samples was analyzed by temperature-programmed reduction (TPR). The experiments were performed in an Ohkura TP-2002S instrument using a mixture of H_2/Ar (5%) as reducing gas. The heating rate was 10 °C/min from room temperature to 900 °C.

The morphology and distribution of the catalytic coatings were characterized by scanning electron microscopy (SEM) JEOL JSM 35C operating at 20 kV, equipped with energy-dispersive system (EDAX). Semi-quantitative results were obtained with the theoretical quantitative method (SEMIQ) of the EDAX software. For the chemical elemental analysis (EDX), the samples were attached with graphite tape onto the sample holder. X-ray spectra were acquired with an accelerating voltage of 20 kV. The sample coating procedures were performed using a combined carbon deposition of metal SPI supplies 12157-AX under argon atmosphere.

A Leica S8 APO stereo-microscope equipped with a Leica LC3 digital camera and LAS EZ software was used for the obtention and processing of the digital images of the foams.

A Testlab TB04 ultrasound bath equipment (40 kHz and 160 W) was used to carry out the stability tests of the catalytic coatings. The weight loss percentage was determined after exposing the samples to an ultrasound bath in acetone at 25 °C for 1 h.

2.4. Catalytic tests

The oxidative dehydrogenation of ethane was carried out in a flow system in a temperature range between 350 and 450 °C. The feed composition was 6% O_2 and 6% C_2H_6 diluted in high purity He. The mass of the catalysts used was about 400 mg and the final flow was fixed to get a constant W/F value of 0.48 g.s/cm^3. Reactants and

Table 1
Nomenclature and characteristics of the prepared catalysts.

Catalyst[a]	Metal loading (wt%)	Co/Ni atomic ratio[b]	NiO crystal size (nm)[c]	Surface area (m^2/g)	Impregnation cycles of active metals	Al_2O_3 weight gain (wt%)[e]
Ni (15) P	15.00	–	12.4	170	–	–
Ni (15) S–CS	13.30	–	–	–	1	13.58
Ni (15) S–DS	14.70	–	–	–	3	13.08
NiCo (15/0.114) P	15.00	0.114	13.1	165	–	–
NiCo (15/0.114) S–CS	15.74[d]	0.114	–	–	1	13.62
NiCo (15/0.114) S–DS	17.30[d]	0.114	–	–	4	12.54
NiCo (15/0.253) P	15.00	0.253	15.8	151	–	–
NiCo (15/0.253) S–CS	15.51[d]	0.253	–	–	2	12.88
NiCo (15/0.253) S–DS	18.30[d]	0.253	–	–	4	15.05

[a] P: powder, S: structured.
[b] Ratio in the solution containing metallic salts: CS – concentrated solution, DS – diluted solution.
[c] Estimated by the Scherrer equation.
[d] Referred to NiO.
[e] Referred to weight gain (wt%) with respect to total mass of the calcined foam.

products were analyzed with a Shimadzu GC 2014 gas chromatograph equipped with a packed column (HayeSep D). In addition, negligible concentrations of carbon monoxide were detected in the products stream after the reaction. Closure of the carbon mass balance was $100 \pm 2\%$. The conversion of ethane ($X_{C_2H_6}$) and the selectivity toward ethylene ($S_{C_2H_4}$) were based on the carbon mass balance and were calculated as follows:

$$X_{C_2H_6} = \frac{[CO] + [CO_2] + 2[C_2H_4]}{2[C_2H_6]} \times 100$$

$$S_{C_2H_4} = \frac{2[C_2H_4]}{[CO] + [CO_2] + 2[C_2H_4]} \times 100$$

The productivity of ethylene was given by the following equation:

$$P = \frac{F_{C_2H_6} \times X_{C_2H_6} \times S_{C_2H_4} \times 28}{W_{Ni}}, \quad (g_{C_2H_4}/kg_{Ni}\ \ h)$$

where $F_{C_2H_6}$ is the flow rate of ethane in mol/h, 28 (g/mol) is the molecular mass of ethylene and W_{Ni} is the mass of Ni (kgNi).

3. Results

3.1. Main features of the structured catalysts

Pieces of the raw foam were conducted to a normalized pretreatment to stabilize the foam walls surface and to generate some roughness to favor the anchorage of the catalytic coating. They were calcined in air at 900 °C for 2 h [11].

In order to produce a γ-Al_2O_3 layer onto the pretreated foam, the substrate was immersed into the colloidal alumina suspension, blown, dried and calcined. At the end of this procedure, the average weight gain was $13.68 \pm 1.40\%$ (Table 1). A homogeneous layer of the support (γ-Al_2O_3) onto the foam walls was obtained. However, some cracks were observed in a few areas, mainly in the most external coating layer (Fig. 1) [16]. These imperfections are related to the calcination and drying process performed for the removal of solvent and the stabilizing agents of the colloidal suspension [17].

The impregnation of the active metallic oxides was carried out following the cycle: immersion–blowing–drying–calcination. This cycle was repeated as many times as necessary to achieve the value of metallic oxide loadings close to 15 wt%. The number of cycles was higher for those samples impregnated with a low concentration solution (Table 1).

To study the coating stability, the structured systems were submitted to an ultrasonic bath. Valentini et al. [18] used this method to evaluate the adherence of γ-Al_2O_3 onto ceramic and metallic supports with petroleum ether as solvent. Banús et al. also performed similar tests by immersion into either acetone or water [17].

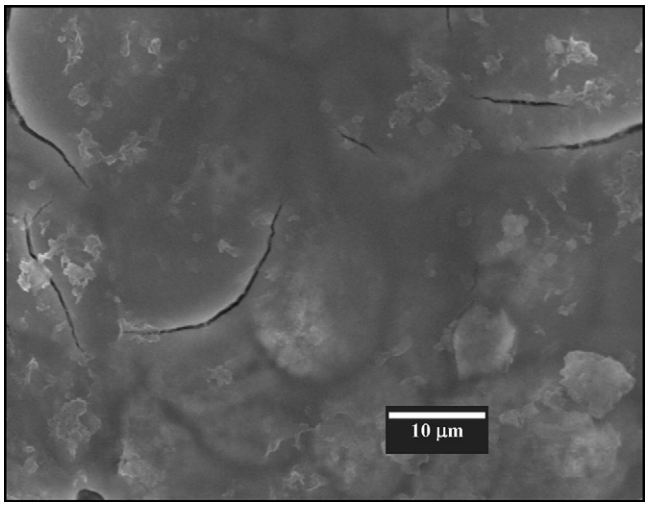

Fig. 1. SEM micrograph of the structured catalyst.

The results are presented in Fig. 2. All systems showed a good adhesion of the catalytic layer deposited over the substrate. The

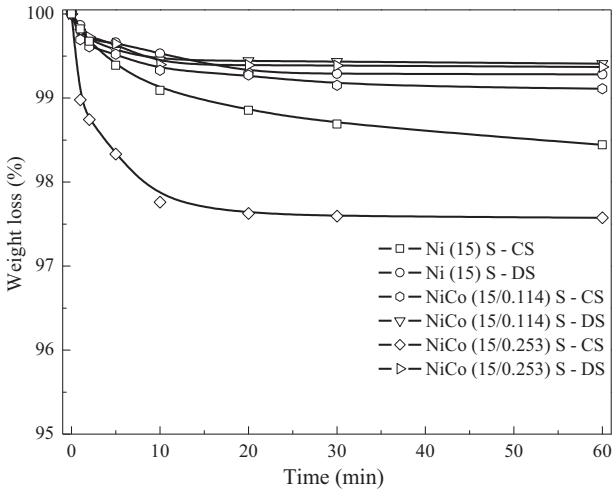

Fig. 2. Stability test for the structured systems: Ni (15) S, NiCo (15/0.114) S and NiCo (15/0.253) S.

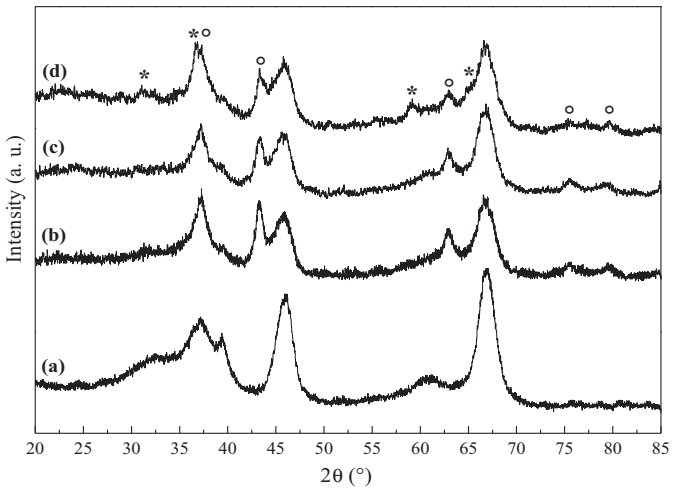

Fig. 3. X-ray diffraction patterns of the powder catalysts: Al_2O_3 (a), Ni (15) (b), NiCo (15/0.114) (c) and NiCo (15/0.253) (d). Symbols: ◦NiO and *Co_3O_4.

maximum weight loss (referred to total mass, foam + coating) was less than 2.5 wt% after 60 min of ultrasonic treatment.

It is important to note that this percentage rose up to around 12.0 wt% if the weight loss achieved with the experiments was referred only to the catalytic coating mass. However, in all cases some foam metal struts were detached from the structure, so the loss of catalytic material resulted considerably lower.

3.2. Main features of the powder catalysts

The support (γ-Al_2O_3) surface area was 249 m^2/g. The addition of active metal oxides led to a decrease of the surface area, being 170 m^2/g for the monometallic oxide catalyst, 165 m^2/g for the catalyst with Co/Ni = 0.114 and 151 m^2/g for the bimetallic oxide system with Co/Ni = 0.253. Moreover, the NiO crystallite sizes obtained from the XRD patterns of the three samples increased while the surface area decreased (Table 1).

3.3. Catalyst characterization: components and active phases

The results of X-ray diffraction corresponding to the powder catalysts are presented in Fig. 3. All diffractograms showed the characteristic peaks of the support, Al_2O_3, (JCPDS: 10-425) and cubic nickel oxide (NiO) at 37.3; 43.3; 62.9; 75.5 and 79.6° (JCPDS: 47-1049). The presence of bulk $NiAl_2O_4$ could not be confirmed by this technique.

In the catalyst with a higher amount of cobalt (NiCo (15/0.253) P) there appeared other signals that could be attributed to cobalt oxide (Co_3O_4): 31.3; 36.9; 59.4 and 65.3° (JCPDS: 42-1467). In addition, the incorporation of this amount of cobalt produced a significant growth in the NiO crystal size (Table 1).

The presence of NiO was also confirmed by temperature-programmed reduction (Fig. 4). For the fresh monometallic oxide catalyst (Ni (15) P), a small peak in the temperature range of 300–390 °C, associated with the reduction of bulk crystalline NiO is visible, which is in line with the above XRD results.

Furthermore, in the zone from 390 to 800 °C, a large and asymmetric broad peak can be seen. In this sense, various reports have postulated the existence of a bi-dimensional species, "surface Ni spinel", with this cation occupying octahedral and tetrahedral sites, where the latter species are harder to reduce than the former [19,20].

The reducibility of the catalyst did not change appreciably after the addition of cobalt with a low ratio (NiCo (15/0.114) P), although

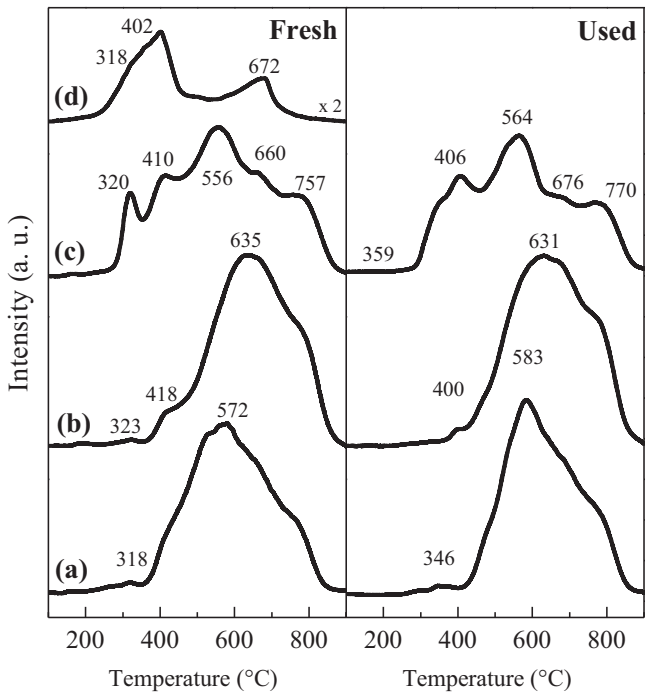

Fig. 4. Temperature-programmed reduction profiles of the mono and bimetallic powder catalysts: Ni (15) (a), NiCo (15/0.114) (b), NiCo (15/0.253) (c) and Co (2.0) (d).

the maximum shifted to a higher reduction temperature. On the other hand, the (NiCo (15/0.253) P) profile shows that the maximum temperature associated with Ni cation reduction is moved to lower values. The presence of new peaks at lower temperatures could be related to the reduction of different cobalt compounds. The former two peaks (~320 and ~400 °C) are probably associated with the two-step reduction process of Co_3O_4 particles to metallic Co, involving CoO formation ($Co^{3+} \rightarrow Co^{2+} \rightarrow Co^0$). This is in agreement with the reduction profile of Co (2.0) P (Fig. 4). The interaction of Co_3O_4 with the support could allow identifying the split of these reduction peaks [21]. A contribution of bulk-like nickel species is also present.

Besides, the new shoulder observed at higher temperatures could be related to amorphous surface layers of cobalt oxides (Co_xO_y), highly dispersed and with a strong interaction with the support. This formed phase would be different from crystalline $CoAl_2O_4$ (not detected by XRD) and would present an intermediate reducibility between cobalt oxides and the bulk spinel [22].

The TPR profiles of the catalysts used in the test reaction were not significantly modified compared to the fresh catalysts, suggesting a high stability of the species after submitting the solids to reaction conditions (Fig. 4).

Fig. 5a shows the Raman spectra of fresh powder catalysts. The spectrum of the monometallic oxide catalyst ((Ni (15) P) spectrum, Fig. 5a) showed a broad band in the region of 500–550 cm^{-1} associated with the stretching of the bond Ni—O (first order phonons). Bulk nickel oxide shows a main signal centered at ~500 cm^{-1} [23]. In this case, the observed shift in the maximum frequency of this band could be associated with the interaction between the alumina and nickel species (support effect) [24,25]. The region of the spectrum at 430–450 cm^{-1} also displayed a small shoulder assigned to the material surface vacancies (non-stoichiometric nickel oxide) [23]. Weak bands at 700 and 1080 cm^{-1} assigned to 2TO and 2LO phononic modes of NiO were visualized [26]. Moreover, there was no evidence of specific bands corresponding to crystalline $NiAl_2O_4$ [24,27].

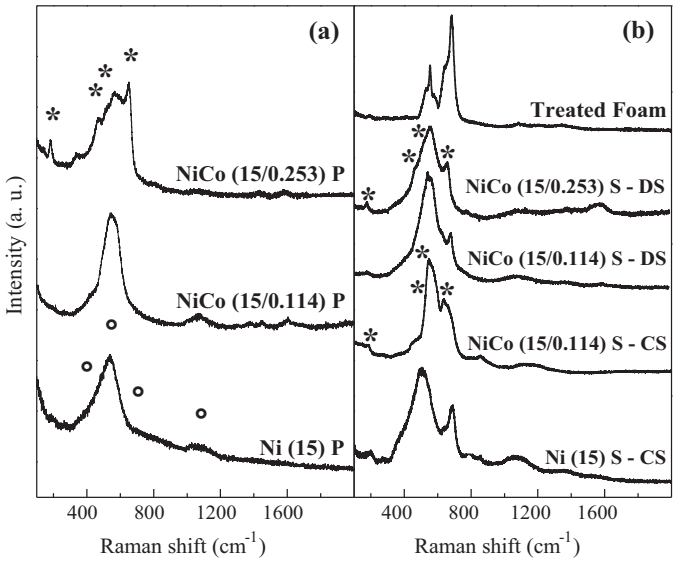

Fig. 5. Laser Raman spectra of the fresh catalysts and treated substrate: powder forms (a) and structured forms (b). Symbols: ◦NiO and *Co_3O_4.

The bimetallic oxide samples also showed the bands corresponding to the Ni—O bond. In addition, the spectrum of the solid with a higher amount of promoter (NiCo (15/0.253) P) showed the characteristic signals corresponding to Co–O at 655, 513, 468 and 187 cm^{-1}. These bands were assigned to Co in octahedral (CoO_6) and tetrahedral (CoO_4) coordination, respectively, with a spinel-type structure. The absence of a medium intensity and sharp band at ~750 cm^{-1} could suggest that crystalline $CoAl_2O_4$ is not present [28–30]. Nevertheless, non extra signals associated with Co–O were observed in the NiCo (15/0.114) P spectrum indicating that Co_3O_4 was absent in this sample. The added Co could be forming a solid solution as Ni(Co)O. In this case, a broad band around 580 cm^{-1} assigned to the Co^{2+}–O stretching mode was expected [31] but, this signal was overlapped by those of Ni—O.

Fig. 5b shows the spectra of fresh mono and bimetallic oxide structured catalysts. For comparison, it also includes the spectrum of pretreated foam. The latter one shows the characteristic vibration modes of the pretreated metallic substrate, mainly between 600 and 800 cm^{-1}. These bands were assigned to chromium, iron and manganese spinels ($FeCr_2O_4$ and $Mn_{1+x}Cr_{1-x}O_{4-x}$) and chromium oxide (Cr_2O_3). These compounds were formed on the surface foam walls after the thermal treatment [11] and they were also present in all structured catalysts.

The Raman signals of the Ni—O species (430–450, 550, 700 and 1080 cm^{-1}) are observed in all the spectra of the structured catalysts (Fig. 5b).

The bands of cobalt spinel could not be identified in NiCo (15/0.114) S–DS. In the other two catalysts (NiCo (15/0.114) S–CS and NiCo (15/0.253) S–DS), these signals appeared with different intensities, somehow suggesting the presence of the cobalt oxides. Instead, these bands were clearly visible in the NiCo (15/0.253) S–DS spectrum, indicating that the cobalt oxide was formed.

Energy-dispersive X-ray analysis allows analyzing the molar ratios of the most representative elements in the coating (Ni, Al, Co and Cr). The results obtained in the different areas analyzed over the covered foams are shown in Table 2.

The monometallic oxide catalyst Ni (15) S–CS showed, in general, a Ni/Al ratio close to the powder sample (Ni/Al = 0.13). Nevertheless, in some sectors, an important enrichment of the active metal was verified. This metallic oxide aggregation was also observed by optical microscopy (Fig. 6). According with the previous results, the system prepared with diluted solution (Ni (15) S–DS) showed a more homogeneous Ni/Al ratio.

Table 2
EDX results of the most representative elements present in the coverage.

Catalyst	Region	Molar ratio				
		Ni/Al	Co/Ni	Co/Al	Cr/Ni	Cr/Al
Ni (15) S–CS	1	0.11	–	–	0.06	0.01
	2	0.13	–	–	0.06	0.01
	3	0.42	–	–	0.05	0.02
	4	0.22	–	–	0.03	0.01
Ni (15) S–DS	1	0.13	–	–	0.05	0.01
	2	0.13	–	–	0.05	0.01
	3	0.16	–	–	0.09	0.01
	4	0.15	–	–	0.05	0.01
Ni Co (15/0.114) S–CS	1	0.09	0.13	0.011	0.15	0.02
	2	0.07	0.15	0.011	0.09	0.01
	3	0.06	0.08	0.005	0.19	0.01
	4	0.06	0.09	0.005	0.12	0.02
Ni Co (15/0.114) S–DS	1	0.21	0.17	0.035	0.04	0.01
	2	0.22	0.13	0.029	0.04	0.01
	3	0.22	0.13	0.029	0.04	0.01
	4	0.22	0.13	0.029	0.04	0.01
Ni Co (15/0.253) S–CS	1	0.08	0.12	0.010	4.09	0.34
	2	0.11	0.35	0.039	0.20	0.02
	3	0.07	0.25	0.018	0.47	0.03
	4	0.06	0.30	0.018	1.02	0.06
Ni Co (15/0.253) S–DS	1	0.15	0.24	0.035	0.22	0.03
	2	0.12	0.28	0.032	0.19	0.02
	3	0.10	0.29	0.031	0.07	0.01
	4	0.15	0.27	0.040	0.05	0.01

On the other hand, in the samples with cobalt, the Co/Ni ratio in some areas of the surface coating was markedly higher than the one presented by the corresponding powder catalyst (Co/Ni = 0.114), which indicates an increase in the percentage of cobalt. It was also noted that in some other areas this ratio was lower, showing a decrease of this metal. This behavior was not so evident in NiCo (15/0.114) S–DS. The Co/Ni and Ni/Al ratios were, in general, more uniform.

The systems with higher amount of cobalt presented similar results when compared with other structured catalysts. We can conclude that the use of the diluted solutions in the impregnation process leads to a better distribution of the active phase.

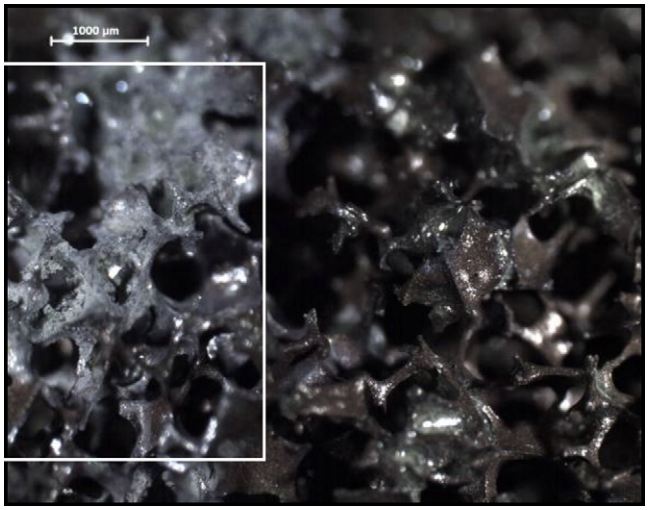

Fig. 6. Image of the used Ni (15) S–CS catalyst obtained with a stereomicroscope. Square: active metal accumulation zone.

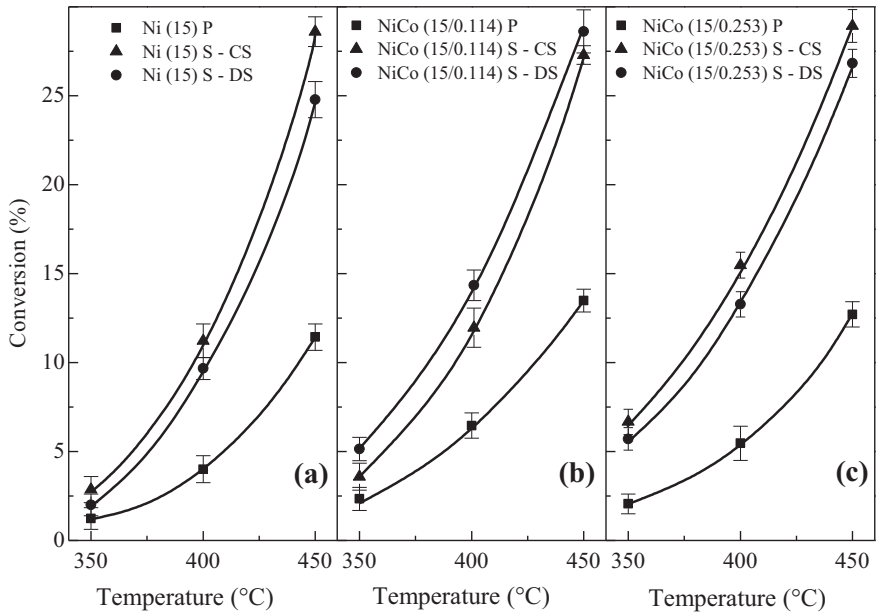

Fig. 7. Ethane conversion of the prepared catalytic systems: (a) Ni, (b) Co/Ni = 0.114 and (c) Co/Ni = 0.253. Reaction conditions: $W/F = 0.48$ g.s/cm^3, $C_2H_6/O_2 = 1$.

The presence of aluminum in all sectors and the relative constancy of the Cr/Al ratio confirmed the quite correct distribution of the support (Al_2O_3) over the foam walls. The enrichment of nickel with respect to the treated substrate (Cr/Ni = 5.53) was evident, indicating that it corresponds to the active phase.

3.4. Catalytic behavior in the oxidative dehydrogenation of ethane

The main reaction is the dehydrogenation of ethane to ethylene in the presence of oxygen, water being a by-product (reaction (1)). In addition, there are other secondary reactions as the total oxidation of the paraffin and/or the olefin formed (reactions (2) and (3), respectively).

$$C_2H_6 + O_2 \rightarrow 2C_2H_4 + 2H_2O, \quad \Delta H = -105\,\text{kJ/mol} \tag{1}$$

$$2C_2H_6 + 7O_2 \rightarrow 4CO_2 + 6H_2O, \quad \Delta H = -1428\,\text{kJ/mol} \tag{2}$$

$$C_2H_4 + 3O_2 \rightarrow 2CO_2 + 2H_2O, \quad \Delta H = -1323\,\text{kJ/mol} \tag{3}$$

Fig. 7 shows the ethane conversion at different temperatures for the powder and structured catalysts. In all cases, a moderate conversion level of ethane was observed (compared with catalytic systems reported in the literature). For powder catalysts, with metallic oxide loading of 15%, the incorporation of Co to the catalytic formulation slightly improved the activity.

Comparing the structured systems with the corresponding powder form, an increase in the conversion values of the former was evident in the three formulations (Fig. 7). Using concentrated and diluted solutions, no significant conversion changes were observed in the monometallic oxide catalyst or in one of the bimetallic oxide structured catalysts (compare the conversion profiles of Ni (15) S–CS with Ni (15) S–DS and NiCo (15/0.253) S–CS with NiCo (15/0.253) S–DS). However, the positive effect of using a precursor diluted solution for the impregnation of the active metallic oxides to the support layer could be observed in the bimetallic oxide structured catalyst NiCo (15/0.114) S–DS (Fig. 7b).

The selectivity to ethylene for all catalysts is presented in Fig. 8. The powder catalysts in general present a higher selectivity than the structured systems. This behavior is less significant for the bimetallic catalysts with a Co/Ni ratio of 0.253 (Fig. 8c). Even so, their selectivities were low for both powder and structured catalysts with this high Co/Ni ratio.

On the other hand, the structured catalysts showed an increase in selectivity when the impregnation solution used in the preparation process was the diluted solution (DS) in comparison with that of the sample prepared with the concentrated ones (CS) (Fig. 8).

The selectivity toward ethylene of the monometallic oxide structured catalyst (Ni (15) S–DS) evaluated at constant temperature (450 °C) and with different W/F ratio showed a decrease as the ethane conversion increased from 18 to 28% (Fig. 9). Whereas under the same reaction conditions, the selectivity for the bimetallic oxide system (NiCo (15/0.114) S–DS) presented almost constant values with the conversion increment (Fig. 9).

The calcined raw foam and the coated foam with Al_2O_3 were also tested under the same reaction conditions. The former presented a negligible activity whereas the latter had a low activity and the only product was CO_2. Some active sites for the total oxidation of ethane are present on the alumina layer due to the component migration of the treated foam toward this layer, such as chromium, iron and manganese spinels ($FeCr_2O_4$ and $Mn_{1+x}Cr_{1-x}O_{4-x}$) [11].

It is worth mentioning that all the catalysts were tested during more than 8 h in reaction stream and no significant modifications in either conversion or selectivity were observed.

According to the ethylene productivity, Fig. 10 shows that at 450 °C the productivity to the main product obtained with the powder samples was similar to the values reported in the literature for Ni-based alumina-supported catalysts [14]. The incorporation of Co with the lower proportion (NiCo (15/0.114) P) resulted in a positive effect for the productivity at 450 °C, while an increase in the Co/Ni ratio the effect is opposite (NiCo (15/0.253) P). It is important to mention that, at the other reaction temperatures (350 and 400 °C), the results obtained showed the same tendency.

The monometallic oxide structured system (Ni (15) S–CS) showed a lower productivity compared to those of the corresponding powder sample. At the same time, Ni (15) S–DS revealed a better value.

The bimetallic oxide structured systems with a low Co/Ni ratio (NiCo (15/0.114) S–CS and NiCo (15/0.114) S–DS) followed the same trend as the above results. An enhancement in productivity was observed when the structured catalyst was prepared with the diluted solution. In this latter case, the active metals showed a

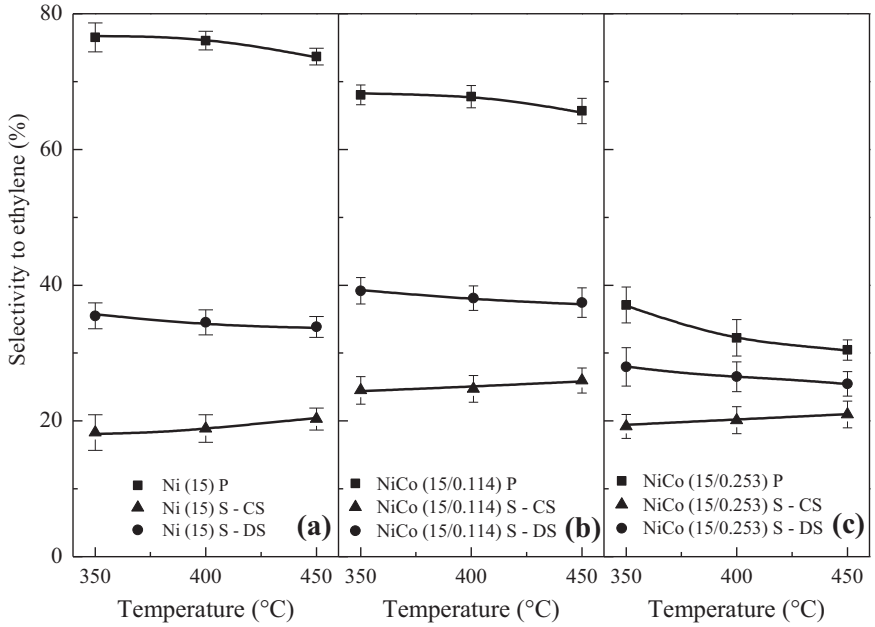

Fig. 8. Selectivity to ethylene of the prepared catalytic systems: (a) Ni, (b) Co/Ni = 0.114 and (c) Co/Ni = 0.253. Reaction conditions: $W/F = 0.48$ g.s/cm^3, $C_2H_6/O_2 = 1$.

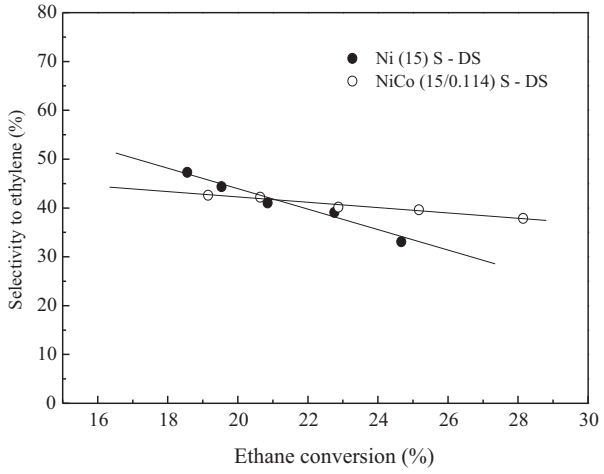

Fig. 9. Selectivity to ethylene as a function of ethane conversion. Reaction conditions: $T = 450\,^{\circ}C$, $C_2H_6/O_2 = 1$.

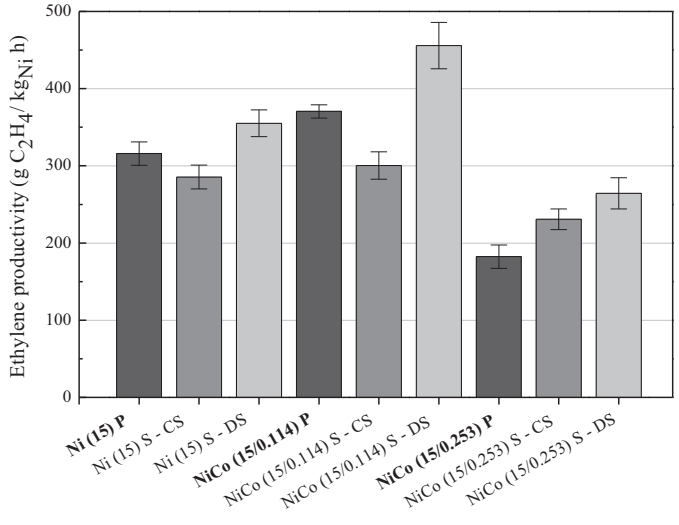

Fig. 10. Ethylene productivity at 450 °C of the prepared systems.

more homogeneous ratio over the foam walls (Table 2). For both catalysts with high Co/Ni ratio (NiCo (15/0.253) S–CS and NiCo (15/0.253) S–DS) the productivity of ethylene resulted higher than the corresponding powder sample. Once more, the structured system prepared with diluted solution showed higher productivity than the one prepared with the concentrated solution. In this case, Co/Ni ratio = 0.253, the powder form had a marked decrease in the selectivity to ethylene.

In brief, the structured catalysts showed an increment in the catalytic activity but with a lower selectivity. Simultaneously, the structured catalysts prepared from diluted solutions (DS) presented better ethylene productivities than the systems prepared with the concentrated ones (CS) (Fig. 10). Moreover, the enhancement on the catalytic performance for the former structured catalysts could be due to their fairly homogeneous Ni/Co ratio and the absence of cobalt oxides aggregations on its catalytic coating.

4. Discussion

4.1. Mechanical stability of the catalytic coatings

The adherence of the catalytic coatings was good for all the structured catalysts so obtained (Fig. 2). A notable reproducibility on the weight loss was observed for those coatings in which the incorporation of the active components was performed using diluted solutions (DS). In these three cases, the weight loss was around 0.7% after 60 min in the ultrasonic treatment. However, the weight loss variation was from 0.9 to 2.4%, when a concentrated precursor solution (CS) was used for active component incorporation. Therefore, concentration of the precursor solution and number of calcinations steps required to achieve the final oxide loadings play a role in the coating stability.

4.2. Metallic oxide species on the powder and structured catalysts

The physicochemical characterizations of the powder samples by TPR and XRD cooperate in the understanding of their Raman spectra. By extension, the analysis of the Raman spectra of the structured catalysts may shed light on their metallic oxide species present on the Al_2O_3 layers.

The existence of the typical XRD signals of NiO in all the powder catalysts suggests the support surface saturation by bi-dimensional Ni species, covering the monolayer and the incipient formation of three-dimensional oxide species. The monolayer coverage of this support is above 12% [19,32]. The presence of these species was confirmed by the TPR results, which indicated the existence of highly dispersed Ni having a strong interaction with the alumina with some amount of bulk Ni oxide. The complex interaction between nickel and the support used in this work might form a spinel-type phase, probably on the surface as nickel aluminate-like species. The latter species were not detected by either LRS or XRD, which is consistent with a surface Ni–Al interaction. The information from the literature about the formation temperature of the bulk $NiAl_2O_4$ spinel is controversial. Some reports suggest that this structure is slowly formed from 600 °C while another ones claim that it is formed around 800 °C [24,25].

The TPR profiles of the powder catalysts did not change substantially after the addition of cobalt in low proportion. This fact suggests that Co is probably well dispersed into the matrix of $NiO–Al_2O_3$ and that, to a certain extent, its presence modifies the nickel distribution and the interaction on the support. The incorporation of a higher loading of cobalt produced the formation of cobalt oxides (clearly identified by XRD and LRS). In this way, the presence of this compound could weaken the interaction with alumina and could contribute to the nickel reduction process, as suggested by the shift to lower values in the reduction temperature of the main peak.

The Raman spectra of all the powder catalysts, in agreement with the TPR and XRD results, indicated the presence of Ni species interacting with the support (shift of the Ni—O stretching mode) and non-stoichiometric nickel oxide. In the particular case of the sample with Co/Ni ratio = 0.253, cobalt spinel (Co_3O_4) was identified in addition to the Ni species mentioned above. Therefore, based on this interpretation, it is possible to identify the species in the different catalytic coatings, using their Raman spectra.

The Laser Raman spectra of structured catalysts revealed similar Ni species compared with the powder forms. The bands assigned to cobalt spinel could not be identified in the system prepared with low cobalt loading and diluted solution (NiCo (15/0.114) S–DS). In contrast, the signals corresponding to Co_3O_4 appeared with different intensities in the spectra of the other two catalytic coatings, NiCo (15/0.114) S–CS and NiCo (15/0.253) S–DS, thus demonstrating that the segregation of the cobalt oxide had occurred. Therefore, the synthesis of a catalytic coating using either a precursor concentrated solution to incorporate the active oxides or a higher Co/Ni ratio than 0.114, brought about the agglomeration of Co, forming bulk Co_3O_4 and limiting the dispersion of Co in the Ni—O structure.

4.3. Oxide species: distribution on the Al_2O_3 layer and their influence on the catalytic behavior

The good selectivity to ethylene obtained with the monometallic nickel oxide formulation in powder form, 73% at 450 °C, is due to the fact that NiO is highly dispersed, having a strong interaction with the support. On the other hand, the presence of bulk NiO favors the total oxidation, CO_2 being the main product [14].

The monometallic oxide structured systems prepared with the concentrated solution (CS) showed a lower productivity compared to that of the corresponding powder catalyst (Fig. 10). At the same time, the sample prepared with diluted solution (DS) revealed a slightly better value.

The EDX analysis can give us some insights about these differences in productivity and selectivity. The nickel species distribution on the Al_2O_3 layer is better on the (Ni (15) S–DS) than on the Ni (15) S–CS (Table 2). Thus, bulk NiO agglomerations were expected to have the latter coating due to the non-homogeneous distribution of the active component.

The incorporation of Co with low proportion (Co/Ni = 0.114) in the powder sample was barely positive for ethylene production (Fig. 10). In this case, the presence of cobalt would improve surface Ni distribution by insertion of Co into the NiO structure forming a solid solution Ni(Co)O as proposed by Nydegger et al. [33].

In order to further understand the role of CoO_x in this reaction, two extra catalyst of Co/Al_2O_3 were prepared with 2.0 and 15 wt%, Co (2.0) P and Co (15) P, respectively. A third catalyst with Co/Ni = 0.114 ratio was prepared by mechanically mixing Co (15) P and Ni (15) P. The powder formulation so obtained was designated as NiCo (15/0.114) P–MM. The catalyst Co (2.0) P showed low performance for oxidative dehydrogenation of ethane, the conversion and the selectivity to ethylene at 450 °C being around 5% and ~25% respectively, while the sample Co (15) P showed higher conversion (17.4%) and lower selectivity (~14%) at 450 °C. As expected the cobalt oxides are good catalysts for total oxidation of the paraffin [34]. On the other hand, the conversion of the mechanical mixture NiCo (15/0.114) P–MM (12.5%) resulted similar to that of Ni (15) P and NiCo (15/0.114) P (Fig. 7). However, the selectivity of the former catalyst was the lowest of these three samples, around ~61% at 450 °C. This behavior supports the fact that the addition of cobalt with low Co/Ni ratio during the co-impregnation process improved the nickel species distribution by forming a solid solution and as a consequence, it produces an increment in the productivity to ethylene (Fig. 10).

In the structured systems, the bimetallic oxide catalyst followed the same trend as the monometallic oxide ones. An enhancement in productivity was observed when the system was prepared with the diluted solution. In this case, the active oxides showed a more homogeneous Co/Ni ratio over the foam walls (Table 2). Besides, the Raman spectra of this sample did not show the signals corresponding to cobalt oxides (Fig. 5b), indicating that the use of an adequate concentration of the precursors could avoid the cobalt oxides segregation.

The addition of a higher amount of Co in powder catalyst (Co/Ni = 0.253) leads to a phase segregation to form the cobalt compounds (Co_3O_4 and $Co_xO_y–Al_2O_3$) and contributes to the drop of productivity toward the preferred product. The final sites obtained with this amount of cobalt (presence of cobalt oxides) and the increment in NiO crystal size (Table 1) would be the reasons to justify the notorious decrease in selectivity and productivity observed in the powder sample. It is well known that cobalt oxides are good agents for oxidation reactions [34], which support the above hypothesis. For the structured catalysts with the high Co/Ni ratio, the productivity of ethylene resulted higher than the corresponding powder sample.

The ethylene selectivity of the structured catalyst with the higher productivity, NiCo (15/0.114) S–DS, remains almost constant as ethane conversion increases, inferring that the active sites have more affinity toward ethane than ethylene. Therefore, the total oxidation of the produced alkene (reaction (3)) is decreased whereas the olefin oxidation occurs in the Ni (15) S–DS (Fig. 9) to some extent.

As a general remark, the structured catalysts showed an increment in the catalytic activity but with a lower selectivity compared with the powder forms. The enhancement of CO_2 production was also established by oxygen consumption. The better selectivity achieved in the structured systems prepared with diluted solutions (DS) instead of concentrated ones (CS) can be partially explained by the active phase distribution (Table 2).

According to the EDX analysis performed in several areas of the different bimetallic oxide catalytic coatings so obtained, a better homogeneous distribution of Ni–Co oxides on the Al_2O_3 layer was produced, when a diluted solution was used to incorporate them.

Nevertheless, enrichment of either Co or Ni oxides in some areas was observed when the incorporation of active phases was made using a concentrated solution. So, the different catalytic behavior of the structured systems could be associated with the distribution of the active components on the Al_2O_3 layer, generating active oxides agglomeration in some areas of the foam walls, as shown in (Fig. 6) and Table 2. The high local concentration of nickel (and/or cobalt) oxides in some areas would be related to the impregnation process, in which there would be an optimal combination between solution concentration and number of impregnation cycles. This combination would affect the agglomeration process.

The presence of bulk metal oxide would favor total oxidation of hydrocarbons (reactions (2) and (3)), contributing to a rapid consumption of oxygen and, consequently, to a poor selectivity. Heracleous et al. [14] and Zhang et al. [35] reported that bulk NiO catalysts exhibit good activity for the reaction under study, although the main product is carbon dioxide. In this sense, some structured catalysts showed a different selectivity behavior compared with the powder formulations. The systems prepared with concentrate solutions (CS) showed a slight increment with temperature. This fact was already observed for bulk NiO [36] and other formulations as Ni-loaded zeolites [37,38]. In this case, this could be explained mainly by two reasons: (i) the use of concentrated solutions favored the metal accumulation onto the alumina layer and as a consequence, the presence of bulk NiO was verified (Fig. 6) and (ii) the other cause could be related to the notorious decrease in the amount of available oxygen, which would be positive for the achievement of a higher selectivity.

An additional effect, specifically the migration of some ions from the treated foam (Fe, Cr and/or Mn) to the alumina layer, should be considered. This diffusion phenomenon would also be negative for the selectivity and was recently observed in other structured systems like VO_x/TiO_2 onto stainless steel plates [39] and Au/CeO_2 catalysts deposited on stainless steel (AISI 304) monoliths [40]. However, the investigation of this behavior needs further research.

In brief, the structured catalysts prepared from diluted solutions (DS) presented better ethylene productivities than the systems prepared with the concentrated ones (CS). Moreover, this performance was slightly enhanced for the Co/Ni = 0.114 sample, in which the main characteristics were the quite homogeneous Co/Ni ratio (EDX) and the absence of cobalt oxides in its catalytic coating (LRS). Therefore, a key factor intimately related to the catalytic performance of the structured catalysts is to obtain a uniform distribution of the Al_2O_3 layer and the active metals onto the substrate walls. Consequently, in order to obtain a good balance between activity and selectivity the active phase agglomeration should be avoided. This correspondence between good selectivity and homogeneous dispersion of active metal species was also observed in powder catalysts.

5. Conclusions

The Ni and $NiCo/Al_2O_3$ powder catalysts were active and selective for the oxidative dehydrogenation of ethane. For this active metal loading (15 wt%), the addition of cobalt with low atomic ratio (Co/Ni = 0.114) produced a slight improvement of the ethylene productivity. However, the addition of a higher amount of this metal (Co/Ni = 0.253) led to a lower productivity, probably due to the presence of cobalt compounds and the increase in the NiO crystal size.

For the reaction test under study, the structured systems showed similar catalytic performance comparing with the corresponding powder forms and they also showed good adhesion of the catalytic layer onto the metallic foams. The inhomogeneity observed in the concentrations of active metals (especially in the systems prepared with concentrated solutions) produced modifications in the activity and mainly in the selectivity of the structured systems.

The features of the resulting structured systems are very sensitive to the variables which involve the deposition method (surface foam treatment, solution concentrations, temperature, etc.). So it is necessary to take into account the control of such parameters in order to achieve good, repetitive depositions of the active components and a correct distribution of the support in the coverage. In the same sense, the achievement of a constant relationship between the used promoters is significant, because, otherwise, the activity and selectivity of these systems could be affected.

Acknowledgements

The authors wish to acknowledge the financial support received from ANPCyT (Grant PME 87-PAE 36985 to purchase the RAMAN Instrument), CONICET and UNL. Thanks are also given to J.M. Zamaro for the BET analysis and Elsa Grimaldi for the English language editing.

References

[1] A. Cybulski, J. Moulijn, Structured Catalysts and Reactors, second ed., Taylor and Francis, Boca Raton, 2006.
[2] A.N. Pestryakov, V.V. Lunin, A.N. Devochkin, L.A. Petrov, N.E. Bogdanchikova, V.P. Petranovskii, Appl. Catal. A: Gen. 227 (2002) 125–130.
[3] N. Gokon, Y. Yamawaki, D. Nakazawa, T. Kodama, Int. J. Hydrogen Energ. 36 (2011) 203–215.
[4] E.D. Banús, M.A. Ulla, E.E. Miró, V.G. Milt, Appl. Catal. A: Gen. 393 (2011) 9–16.
[5] C.Y. Zhao, T.J. Lu, H.P. Hodson, J.D. Jackson, Mater. Sci. Eng. A 367 (2004) 123–131.
[6] L. Giani, G. Groppi, E. Tronconi, Ind. Eng. Chem. Res. 44 (2005) 4993–5002.
[7] L. Giani, G. Groppi, E. Tronconi, Ind. Eng. Chem. Res. 44 (2005) 9078–9085.
[8] D. Lehmhus, J. Banhart, Mater. Sci. Eng. A 349 (2003) 98–110.
[9] O. Sanz, L.C. Almeida, J.M. Zamaro, M.A. Ulla, E.E. Miró, M. Montes, Appl. Catal. B: Environ. 78 (2008) 166–175.
[10] L.M. Martínez, T.O. Sanz, M.I. Domínguez, M.A. Centeno, J.A. Odriozola, Chem. Eng. J. 148 (2009) 191–200.
[11] J.P. Bortolozzi, E.D. Banús, V.G. Milt, L.B. Gutierrez, M.A. Ulla, Appl. Surf. Sci. 257 (2010) 495–502.
[12] T. Ren, M.K. Patel, K. Blok, Energy 33 (2008) 817–833.
[13] F. Cavani, N. Ballarini, A. Cericola, Catal. Today 127 (2007) 113–131.
[14] E. Heracleous, A.F. Lee, K. Wilson, A.A. Lemonidou, J. Catal. 231 (2005) 159–171.
[15] B. Solsona, F. Ivars, A. Dejoz, P. Concepción, M.I. Vázquez, J.M. López Nieto, Top. Catal. 52 (2009) 751–757.
[16] J.P. Bortolozzi, E.D. Banús, L.B. Gutierrez, M.A. Ulla, Av. Ciencias e Ing. 2 (2011) 79–87.
[17] E.D. Banús, V.G. Milt, E.E. Miró, M.A. Ulla, Appl. Catal. A: Gen. 362 (2009) 129–138.
[18] M. Valentini, G. Groppi, C. Cristiani, M. Levi, E. Tronconi, P. Forzatti, Catal. Today 69 (2001) 307–314.
[19] Z. Xu, Y. Li, J. Zhang, L. Chang, R. Zhou, Z. Duan, Appl. Catal. A: Gen. 210 (2001) 45–53.
[20] A. Cimino, M. Lo Jacono, M. Schiavello, J. Phys. Chem. 79 (1975) 243–249.
[21] B. Jongsomjit, J. Panpranot, J.G. Goodwin Jr., J. Catal. 204 (2001) 98–109.
[22] D. Schanke, S. Vada, E.A. Blekkan, A.M. Hilmen, A. Hoff, A. Holmen, J. Catal. 156 (1995) 85–95.
[23] S.-H. Lee, H.M. Cheong, N.-G. Park, C.E. Tracy, A. Mascarenhas, D.K. Benson, S.K. Deb, Solid State Ionics 140 (2001) 135–139.
[24] S.S. Chan, I.E. Wachs, J. Catal. 103 (1987) 224–227.
[25] A.V. Ghule, K. Ghule, T. Punde, J.-Y. Liu, S.-H. Tzing, J.-Y. Chang, H. Chang, Y.-C. Ling, Mater. Chem. Phys. 119 (2010) 86–92.
[26] W. Wang, Y. Liu, C. Xu, C. Zheng, G. Wang, Chem. Phys. Lett. 362 (2002) 119–122.
[27] M.A. Laguna-Bercero, M.L. Sanjuán, R.I. Merino, J. Phys.: Condens. Matter 19 (2007) 186217–186227.
[28] B. Jongsomjit, J.G. Goodwin Jr., Catal. Today 77 (2002) 191–204.
[29] J. Jiang, L. Li, Mater. Lett. 61 (2007) 4894–4896.
[30] C.-W. Tang, C.-B. Wang, S.-H. Chien, Thermochim. Acta 473 (2008) 68–73.
[31] M.A. Ulla, R. Spretz, E. Lombardo, W. Daniell, H. Knözinger, Appl. Catal. B: Environ. 29 (2001) 217–229.
[32] X. Wang, B. Zhao, D. Jiang, Y. Xie, Appl. Catal. A: Gen. 188 (1999) 201–209.
[33] M.W. Nydegger, G. Couderc, M.A. Langell, Appl. Surf. Sci. 147 (1999) 58–66.

[34] L. Gutierrez, M.A. Ulla, E.A. Lombardo, A. Kovács, F. Lónyi, J. Valyon, Appl. Catal. A: Gen. 292 (2005) 154–161.
[35] X. Zhang, Y. Gong, G. Yu, Y. Xie, J. Mol. Catal. A: Chem. 180 (2002) 293–298.
[36] Y. Schuurman, V. Ducarme, T. Chen, W. Li, C. Mirodatos, G.A. Martin, Appl. Catal. A: Gen. 163 (1997) 227–235.
[37] X. Lin, C.A. Hoel, W.M.H. Sachtler, K.R. Poeppelmeier, E. Weitz, J. Catal. 265 (2009) 54–62.
[38] X. Lin, K.R. Poeppelmeier, E. Weitz, Appl. Catal. A: Gen. 381 (2010) 114–120.
[39] A. Löfberg, T. Giornelli, S. Paul, E. Bordes-Richard, Appl. Catal. A: Gen. 391 (2011) 43–51.
[40] L.M. Martínez, T.O. Sanz, M.A. Centeno, J.A. Odriozola, Chem. Eng. J. 162 (2010) 1082–1090.